

# Study of Sputtered Barium Strontium Titanate Films for Energy Harvesting Applications

Mariya Aleksandrova<sup>1,\*</sup>, Tatyana Ivanova<sup>2</sup>, Sascha Koch<sup>3</sup>, Frank Hamelmann<sup>3</sup>, Daniela Karashanova<sup>4</sup>, Kostadinka Gesheva<sup>2</sup>

<sup>1</sup>Department of Microelectronics, Technical University of Sofia, 8, Kliment Ohridski Blvd., 1000 Sofia, Bulgaria

<sup>2</sup>Central Laboratory of Solar Energy and New Energy Sources, Bulgarian Academy of Sciences, 72 Tsarigradsko Shosse Blvd., 1784 Sofia, Bulgaria.

<sup>3</sup>Physics of Supramolecular Systems and Surfaces, Faculty of Physics, Bielefeld University, 33615 Bielefeld, Germany

<sup>4</sup>Institute of Optical Materials and Technologies, Bulgarian Academy of Sciences, 109, Acad. G. Bontchev Str. 1113 Sofia, Bulgaria

\*Corresponding author. E-mail: m\_aleksandrova@tu-sofia.bg; Tel.: (+359) 2965 30 85

DOI: 10.5185/amlett.2020.101567

Thin films of BaSrTiO<sub>3</sub> (BST) were deposited by radio frequency (RF) sputtering with sputtering voltage varied between 0.5 and 0.7 kV. BaSrTiO<sub>3</sub> films are investigated regarding their suitability for use in flexible energy harvesting devices. Analysis of the spectra and micrographs showed the piezoelectric features and the polycrystalline nature for the films grown at higher sputtering voltage. Meanwhile, the presence of an amorphous phase with a lack of characteristic bonds was found out for BaSrTiO<sub>3</sub> films grown at the lower sputtering voltage. The electrical measurements of Al/BaSrTiO<sub>3</sub>/Al harvester on plastic substrate in the low-frequency range revealed superior piezoelectric voltage and 40% exceeding power density for the samples prepared at 0.7 kV as compared to the other thin films deposited at 0.5 kV. These results are achieved by simple architecture of single layer harvester with small size (0.4 cm<sup>2</sup>) and small film thickness (0.5 μm), containing lead-free material. It was proved that the sputtered BaSrTiO<sub>3</sub> films are suitable for thin film piezoelectric nanogenerators and their performance could be easily tuned by the sputtering voltage. Possible applications of the proposed element are low-frequency vibrational harvesting and a strain gauge.

## Introduction

In recent years, piezoelectric energy harvesting devices put focus on the study of piezoelectric oxide material properties as the most effective among the piezoelectric materials (ceramics and polymers) [1-3]. BaTiO<sub>3</sub> films, with its high piezoelectric module and possibility to be produced by conventional deposition technologies, have become preferable lead-free material for piezoelectric MEMS devices, sensors, resonators, actuators, and energy harvesting [4-6]. However, making films thinner, piezoelectric material with greater lattice asymmetry is needed to compensate dipoles quenching due to the short distance between the opposite charges. Therefore, suitable material, close to BaTiO<sub>3</sub> in nature, but with enhanced piezoelectric properties has become barium strontium titanate (BaSrTiO<sub>3</sub> or BST) [7]. BST thin nanosized films can be deposited by conventional microfabrication technology on silicon, making it compatible with the MEMS design flow. With the development of the energy harvesting market, BST films have to be used in flexible nanogenerator devices, requiring cyclic applied continuous mechanical loading with low frequency for proper work [8]. However, the available studies reveal only data about material conductivity, behaviour in composition with polymers or resins, flexoelectricity and some relations between charge and pressure [9,10]. Our group has recently prepared and investigated simple

generator with sputtered BST films and established the optimal deposition conditions for obtaining uniform films with controllable thickness, but only impedance spectroscopy and dielectric characterization of the structures was conducted until now [11]. Some of the well-studied properties of BST films and composites are permittivity and leakage related to energy storage applications [12], or capacitance and loss tangent for varactors [13]. Literature data of BST deposited by methods such as sputtering exhibit a great degree of variation in the reported properties. It is thus important to determine the degree to which film microstructure, chemical composition and surface morphology affect the tunable piezoelectric device properties in terms of energy harvesting applications.

In this study, the relations among the BST films' microstructure, functional groups, electronic state of elements and surface morphology, the charge generation ability, produced power with respect to the deposition conditions are investigated. The results showed that the sputtered barium strontium titanate films not only exhibited piezoelectric properties but also their properties are very sensitive to the deposition conditions and respectively they can be tailored by a simple tuning the sputtering voltage. In this way, it is possible to produce superior power density as compared to other reported piezoelectric harvester with similar design and involving lead-free materials. In addition, the enhanced parameters

are produced from a smaller thickness of the piezoelectric films at comparable and even smaller sizes of the harvester. These films are found to be suitable for applications like energy harvesting devices. Similar studies have not been carried out and published yet, up to our knowledge.

## Experimental

### Materials/ chemicals details

The BaSrTiO<sub>3</sub> thin films were deposited on silicon substrates (purchased from SilTronix ST) for the needs of the spectroscopic measurements by radio frequency (RF) sputtering without additional oxidation, using a 99.99% pure composite target with equal portions of barium titanate and strontium titanate (purchased from K. Lesker). This is necessary to avoid contribution of the polymeric substrate having a complex composition to the signal being interpreted. For the needs of the mechanical testing, thermal resistant plastic substrates of polyethylene naphthalate (PEN) were used (purchased from Good fellow).

### Characterizations/device fabrications/response measurements

Before sputtering, the silicon substrates were cleaned in a diluted aqueous solution of hydrofluoric acid for native silicon oxide removal. Then, Si wafers were treated using an ultrasonic bath in acetone, ethyl alcohol and distilled water for 6 min. PEN substrates were cleaned by sonication in acetone for 180 s. Additionally, they were treated in UV/ozone environment for 2 min.

For generated piezoelectric voltage and current measurements, aluminium thin films were grown as a bottom electrode by thermal evaporation. The chamber for sputtering was evacuated to a vacuum level of 10<sup>-6</sup> Torr. The specific deposition conditions were as follow: sputtering pressure was 2.10<sup>-2</sup> Torr, various plasma voltages in the range 0.5-0.7 kV were set and the plasma current values were between 80 and 110 mA (sputtering power ranged approximately between 40 and 80 W), defining sputtering rates of, respectively 8 – 10 nm/min. The temperature inside the chamber was measured by an infrared pyrometer that measures the temperature of the substrate surface through the observation window of the chamber. The films' thickness was measured by alpha-step profiler to be between 400 and 520 nm. One and the same deposition conditions were used for the growth of BST films on the two types of substrates. Top electrodes were prepared also by thermal evaporation of aluminium and were segmented by a shadowing mask at 1 A per 10 s. Five segments, each with dimensions of 0.2 x 0.4 cm, were obtained on the top, thus defining the active piezoelectric areas.

The identification of the chemical bonds and functional groups was performed by Fourier-transform infrared spectroscopy (FTIR) in transmission mode. FTIR spectra were recorded by a Shimadzu spectrophotometer

IRPrestige-21. Scanning electron microscopy was conducted by SEM microscope Philips 515. The electronic state analysis of the BST films was conducted by carrying out X-ray photoelectron spectroscopy (XPS), using an Omicron Multiprobe system consisting of a monochromatic X-ray source (Al K $\alpha$ ) and a hemispherical electron analyser (Omicron SPHERA). The base pressure was 1E<sup>-10</sup> mbar. The spectra data were processed and analysed using the CasaXPS program. XPS was measured at the surface and after 20 min and 40 min of sputtering (or etching) to scan the sub-surface layers in depth. The mechanical load was applied from laboratory-made shaking setup by mounting on trapezoidal beam for uniform distribution of the dynamic stress along the whole sample independently of its area. Vibrations with frequency up to 50 Hz and intensity of 35 N (~9 N/cm<sup>2</sup>) were applied. Details about the mechanical test system and the way of sample mounting are provided elsewhere [14].

Oscillograms were recorded with digital oscilloscope Tektronix TDS 1012B and the current through the samples was measured by high-resolution pico-amperemeter Keithley 6485. All electrical measurements for determination of the intrinsic properties of the harvester (assigned to the materials and films interfaces involved) were conducted at room temperature without load resistance.

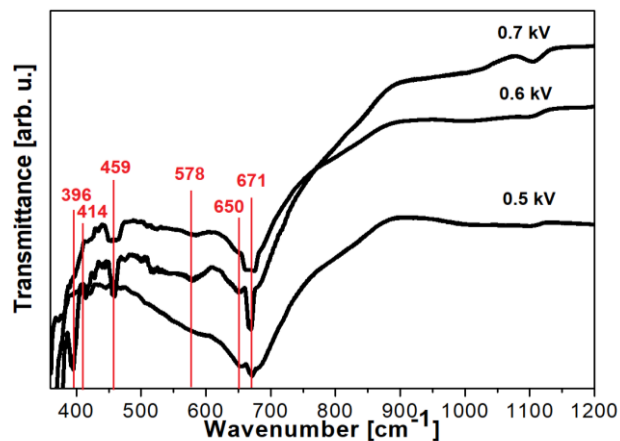


Fig. 1. FTIR spectra of BaSrTiO<sub>3</sub> films sputtered at different sputtering voltages.

## Results and discussion

FTIR spectra were recorded for the BST films, sputtered at different conditions (see Fig. 1). The weak bands seen at 3600 cm<sup>-1</sup> - 3700 cm<sup>-1</sup> and at 2340-2350 cm<sup>-1</sup> are ascribed to the stretching vibrations of hydroxyl groups, due to surface adsorbed water and C=O stretching modes, respectively [15]. The other observed characteristic bands below 2000 cm<sup>-1</sup> and their assignments are described in Table 1. It could be noted that some typical absorption features for the barium titanate lattice, reported also as fundamental for barium strontium titanate, appeared in the BST films grown at sputtering voltage 0.7 kV, but they are not revealed in the films prepared at lower voltages of

0.5 kV and 0.6 kV. For example, the IR lines at  $476\text{ cm}^{-1}$  (Ti-O stretching mode in  $\text{SrTiO}_3$ ) and at  $517\text{ cm}^{-1}$  (related to Ti-O stretching vibrations along the polar axis in  $\text{BaTiO}_3$ ).

In summary, the intensity of the FTIR absorption band increased with increasing the sputtering voltage that can be related to the substrate temperature increase, as well. This may be due to the ad-atom mobility at higher temperature, which improves the crystallinity of the films and their piezoelectric response. This will be further confirmed by the SEM study and electrical characterization of the harvester samples, involving BST films deposited at the three sputtering voltages. Also, some important features facilitating the piezoelectric effect like stretching bonds along the polar axis in  $\text{BaTiO}_3$  appeared at the higher sputtering voltage ( $517.1\text{ cm}^{-1}$ ). Other unwanted features that suppress the piezoelectric effect in this case of mechanical testing, such as longitudinal modes of  $\text{SrTiO}_3$  structure ( $467\text{ cm}^{-1}$ ), disappeared at the higher sputtering voltage, which is favourable for the energy harvesting behaviour.

In Fig. 2, the XRD patterns of BST films deposited are shown as a function of sputtering voltage. From this figure, when the sputtering voltage is higher or equal to 0.7 kV, a crystalline film has been identified as a perovskite structure (the presence of a strong peak at  $2\theta = 33^\circ$ ). However, when the sputtering voltage is lower than 0.6 kV, the perovskite structure cannot be formed and this peak lacks.

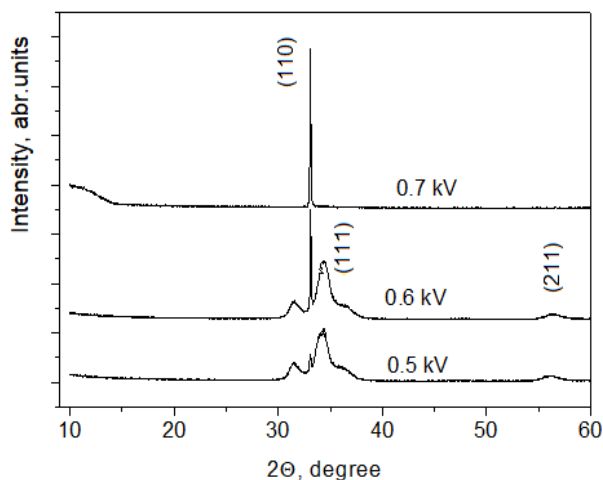


Fig. 2. XRD patterns of BST films sputtered at various voltages.

Since the sputtering voltage, respectively sputtering power is related to the temperature revealed at the substrate due to self-heating from the plasma, then it can be concluded that the revealed temperature of  $190^\circ\text{C}$  is responsible for the stronger crystallization of the film produced at 0.7 kV and results in the development of cubic perovskite structure (110). It is observed that after sputtering at 0.6 kV, the (110) peak from the BST film became less sharp and its intensity decreased, which is evidence for the lower degree of crystallization as

compared to the film grown at 0.7 kV. The results are in good agreement with the reported in [21].

Table 1. Description of the position and interpretation of FTIR absorption bands of  $\text{BaSrTiO}_3$  films.

| Absorption band positions |                    |                    | Assigned to   |
|---------------------------|--------------------|--------------------|---|
| 0.5 kV                    | 0.6 kV             | 0.7 kV             |   |
|                           |                    | 1107.9 weak        | Indication of formation of Si-O- $\text{BaTiO}_3$ and Si-O-Si bonds [16]                    |
| 667.7 strong broad        | 671.8 strong broad | 668.5 strong broad | Ti-O stretching [16]  |
| 647.6 shoul-der           | 652.4 clear        | 650.8 clear        | Ti-O bending mode in $\text{BaTiO}_3$ [15]  |
| 579.1 weak broad          |                    | 578.2 clear        | Ti-O characteristic for perovskite formation, Ti-O stretching mode of $\text{BaTiO}_3$ [16] |
|                           |                    | 517.1 clear        | Ti-O stretching along the polar axis in $\text{BaTiO}_3$ with tetragonal phase [17]         |
|                           |                    | 476.0 weak         | Ti-O stretching $\text{SrTiO}_3$ [18]   |
| 467 weak                  | 467 weak           |                    | Longitudinal modes of $\text{SrTiO}_3$ structure [19]                                       |
| 459.1 clear               |                    | 459.1 clear        | Ti-O stretching $\text{BaTiO}_3$ [18]   |
|                           |                    | 413.9 clear        | Ti-O bending modes  |
|                           |                    | 396 very clear     | $\text{TiO}_6$ and Ti-O bending vibrations [20]   |

A change in the (100) peak positions (where present), to the lower angle as compared to pure  $\text{BaTiO}_3$  could be noted, indicating an increase in the value of the lattice parameter due to Sr substitution in the barium titanate lattice, similar to all elements with an ionic radius larger than  $\text{Ti}^{4+}$ . This pattern indicates the presence of a phase associated with the large asymmetry of the crystal, as shown by the crystallographic orientation, suggesting a stronger piezoelectric response, as compared with the case of the film sputtered at 0.5 kV [22].

The surface morphology of the BST thin films is studied by SEM technique and the images are shown in Fig. 3. All films exhibited flat surface morphology with small grains. Larger, more visible and well defined are the grains in the case of BST films, deposited at 0.7 kV, due to the formation of crystalline phase of  $\text{BaSrTiO}_3$ , as it is proved by the other analyses of the films. All samples were characterized with relatively defectless surfaces without micro-cracks, or micropores, or other microdefects, as can be seen from the SEM images. This is beneficial for obtaining good surface contact properties at the interface with the electrode film. However, in the same manner, as in the FTIR spectra, evolution of the films' crystallinity could be observed with the sputtering voltage increase. SEM images of the samples show the change of the film surface morphology with the sputtering voltage applied.

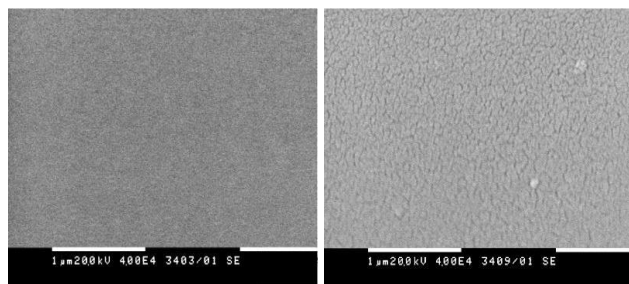


Fig. 3. SEM micrographs of BaSrTiO<sub>3</sub> films sputtered at (a) 0.5 kV; (b) 0.7 kV.

The surface morphology is evolved from a non-granular surface of the film deposited at 0.5 kV (Fig. 3a), transformed into a small-sized granular film, obtained at 0.7 kV (Fig. 3b). The results are in good agreement with reported data for sputtered undoped barium titanate, having the same cubic perovskite structure and similar chemical composition [23]. The reason for the observed microstructural change could be ascribed to the temperature increase during the thin film deposition, as the sputtering voltage difference of 200 V in the vacuum chamber corresponds to a temperature difference of more than 80°C which could contribute for the crystallites formation. It seems that the films with the granular structure exhibited more of the groups and bonds typical for perovskite structure as was proved with the FTIR study and respectively they can show piezoelectric properties. Thus, it is expected stronger piezoelectric response from these samples.

Considering the results from FTIR, XRD and SEM, further XPS study was conducted only on the sample, prepared at sputtering voltage 0.7 kV. The results are presented in Figs. 4a-e.

The XPS spectra confirm the presence of Ba, Ti, Sr, O and C elements in the film structure. The carbon components in the magnetron sputtered films can be attributed to contamination, which resulted from the samples being exposed to the ambient atmosphere and/or the oil diffusion pump during the sputtering process [24]. The carbon peaks closed at 286.10 and 289.81 eV appeared in the spectra and gradually diminish with etching and after 40 min etching, there is no carbon detection into the film structure. The C 1s signal has two components attributed to C-O bond (286.10 eV) and to BaCO<sub>3</sub> (289.81 eV) [25]. The presence of BaCO<sub>3</sub> is evident from the Ba and O signals as well.

The O 1s line consists of three contributions on the surface layer and after 20 minutes of etching. After Ar etching for 40 min, the contribution from 531.8 eV is not detected. The binding energy of O 1s at 531.8 eV may be related to the carbonate species or to hydroxyl groups typical for absorbed water. FTIR analysis reveals very weak absorption bands due to hydroxyl groups' vibrations, but in this case, this component at 531.8 eV is related to carbonate presence and it vanishes along with the carbon signal. The low binding energy peak around 530.3-530.9 eV is usually assigned to metal oxide. This peak is

attributed to O<sup>2-</sup> ions in BaSrTiO<sub>3</sub> phases [26], the other peak at 532.5 eV can be due to an oxidation state O<sub>x</sub> (0 < x < 2), connected with chemisorbed species, oxygen vacancies and to the non-perovskite structure of BST [27].

XPS spectra of Ba 3d are consisted from the doublets with the binding energies at 779.5 eV and 795.7 eV assigned to Ba 3d<sub>5/2</sub> and Ba 3d<sub>3/2</sub> lines, respectively. Each of the Ba 3d<sub>3/2</sub> and Ba 3d<sub>5/2</sub> peaks can be decomposed in two peaks, which indicated that barium, is in different chemical states.

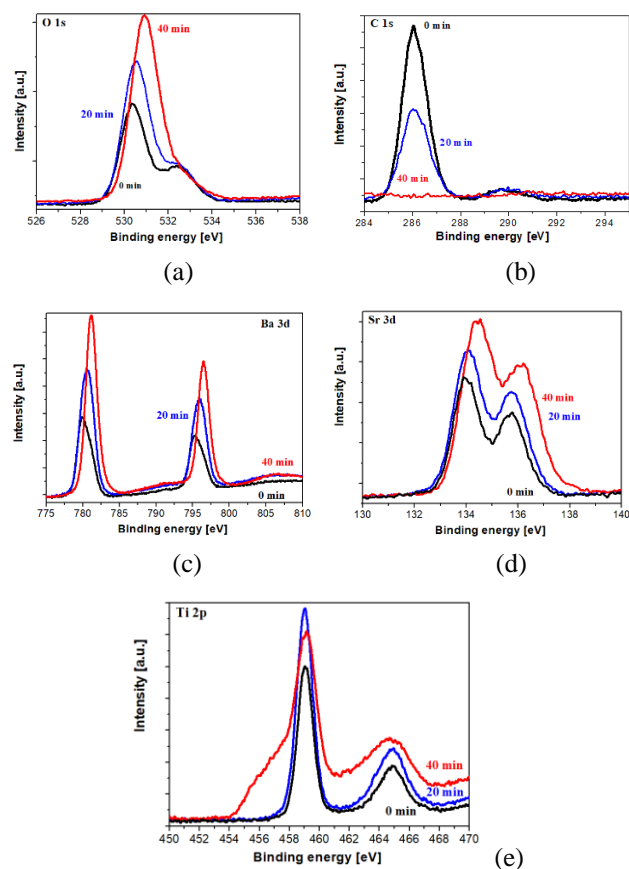


Fig. 4. XPS study of BaSrTiO<sub>3</sub> film sputtered at 0.7 kV, performed on the film surface and after Ar<sup>+</sup> etching for 20 and 40 min.

The similar presence of two different types of Ba atoms in the BaSrTiO<sub>3</sub> films grown by sol-gel, RF-sputtering, has been revealed in other studies [28]. The lower binding energy pair 795.04 and 779.78 eV can be assigned to Ba atoms in perovskite phase [29]. The other doublet at 795.86 and 781.0 eV are often related to BaCO<sub>3</sub>, or to a relaxed non-perovskite phase due to the oxygen vacancies and the cation defects [30]. The presence of BaCO<sub>3</sub> can be considered for the surface layers, but the C 1s spectrum after 40 minutes etching clearly shows that the carbon is not present, so the line at the binding energy of 781.0 eV is related to the non-perovskite barium strontium titanate phase.

The Sr 3d spectra exhibit a doublet consisting of two symmetrical photoelectron components: Sr 3d<sub>5/2</sub> at binding energy around 134.0 – 134.4 eV and Sr 3d<sub>3/2</sub> at

135.77-136.2 eV. Similar binding energies for Sr 3d line have been reported for SrTiO<sub>3</sub> films [31]. The Ti 2p spectra show asymmetric shapes that can lead to the suggestion that Ti element in the sputtered BaSrTiO<sub>3</sub> film has existed in different chemical states. The Ti 2p signal measured on the film surface and after etching for 20 and 40 min. can be fitted with two peak doublets: the peaks located at lower binding energies 457.7 and 463.4 eV can be ascribed as Ti<sup>3+</sup> valance state, the higher binding energies 459.02 and 464.72 eV are related to Ti<sup>4+</sup>, respectively [32]. It is clearly seen that Ti<sup>3+</sup> 2p<sub>3/2</sub> at 457.12 eV becomes more pronounced after 40 min. Ar etching. The values closed to 458.02 and 459.14 eV, as well as the 464.77 eV are reported for Ti 2p photoelectron spectra for perovskites and BaTiO<sub>3</sub> [33]. The existence of different oxidation states of titanium is related to the oxidation state of oxygen O<sub>x</sub><sup>-</sup> (0 < x < 2) [34].

Quantitative analysis of the elemental composition in the BaSrTiO<sub>3</sub> films was made and the results for 0, 20 and 40 min of sputtering for etching were summarized in Table 2.

**Table 2.** Atomic percentage concentration of the elements in BST film sputtered at 0.7 kV after 0, 20 and 40 min of etching.

|                               | Ti 2p | O 1s  | Ba 3d | Sr 3p | C 1s  |
|-------------------------------|-------|-------|-------|-------|-------|
| % Atomic Concentr.–<br>0 min  | 10.04 | 31.16 | 14.79 | 14.52 | 29.49 |
| % Atomic Concentr.–<br>20 min | 12.03 | 40.28 | 15.34 | 16.88 | 15.47 |
| % Atomic Concentr.–<br>40 min | 15.78 | 40.00 | 16.87 | 17.94 | 9.41  |

The distribution of the atomic concentration of elements from the surface to the depth of the studied BST film showed that at the surface absorption of contaminations take place, which can explain the great percentage of carbon, which however decreased with the layer-by-layer removing. The presence of the carbon after sputtering 40 min was more than 3 times lower, but still existed, which can be ascribed to exhaust from the oil pump during the vacuum deposition process [35]. Regarding the ratio of the Ba and Sr in the total composition, it matches the composition ratio of the sputtering target (although the atomic percentage of Ba and Sr in the target is equal, here the deviation is due to the measurement error of the instrument). This is proof for suitable growth mode, which doesn't change the stoichiometry of the film. The distribution of the useful components is quite similar after 20 min and 40 min of etching, which is evidence for uniform chemical composition across the sample.

To demonstrate the piezoelectric behaviour of the BaSrTiO<sub>3</sub> films produced at different sputtering voltages, a simple flexible energy harvesting element was designed and fabricated, involving piezoelectric films sputtered at 0.5 kV and 0.7 kV and generated voltage was measured. The electromechanical testing was performed in cantilever beam mode with a laboratory-made vibrational setup. The oscillograms presented in figure 5 are related to vibration

with a frequency of 50 Hz applying mass loading equivalent to 100 g/cm<sup>2</sup>.

To characterize the intrinsic conversion ability of the piezoelectric generators and to make possible a comparison between different fabrication conditions, the power output is most commonly measured through the product of the open-circuit voltage and short circuit current [36]. The open-circuit voltage is requested for precise peak detection at the input of the power management integrated circuits [37]. It should be noted that the root-mean-square (RMS) value of the AC electrical signals is significant for the output energy estimation, therefore no matter of the similar peak voltages for BST films produced at 0.5 kV and 0.7 kV, the comparison is made based on RMS voltages and currents.

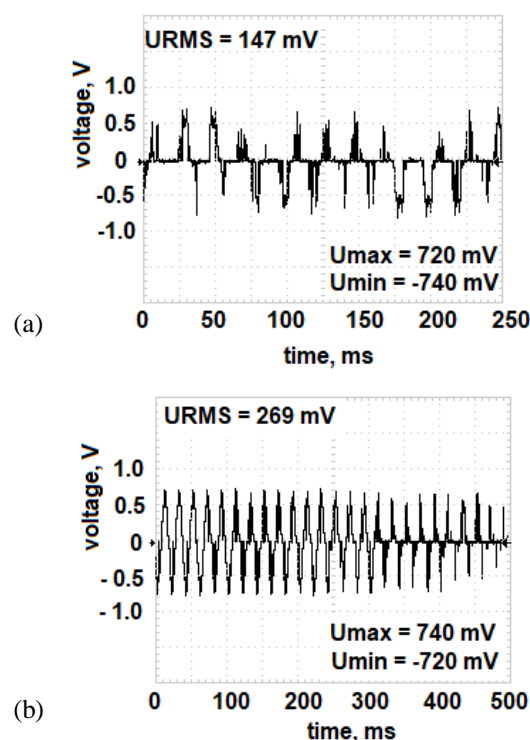


**Fig. 5.** Oscillograms of the produced piezoelectric voltage from flexible energy harvesting devices with BaSrTiO<sub>3</sub> films sputtered at: a) 0.5 kV and b) 0.7 kV.

While the crystalline films with typical perovskite piezoelectric features can produce periodical signal with high symmetry (Fig. 5b: U<sub>max</sub> = 740 mV; U<sub>min</sub> = -720 mV), the less crystalline film lacking most of the piezoelectric phase bonds produced ~100 mV lower voltage with lack of periodicity (Fig. 5a). Although the symmetry of the pulses and their magnitude seems the same in value like the signal from the crystalline BaSrTiO<sub>3</sub> film, the width of the pulses has random distribution, the non-linear distortions are dominant and the RMS value of the voltage is significantly lower. Additionally, the current is lower than 200 nA/cm<sup>2</sup>, with poor dependence on the strain, probably due to dipoles' compensation. This resulted in a decrease of the power output to practically unuseful values.

To estimate the ability of both types of elements to harvest and convert mechanical to electrical energy after applied strain, the produced electrical power densities were compared (Fig. 6). Although similar behaviour could be noted for both films (maximum produced power at 10% strain, decreasing to 20%), the power density for energy harvesting with BaSrTiO<sub>3</sub> sputtered at 0.7 kV showed 40% higher maximum power density. The results are in good agreement with the recently reported [38] and these values are typical for the piezoelectric thin film nanogenerators.

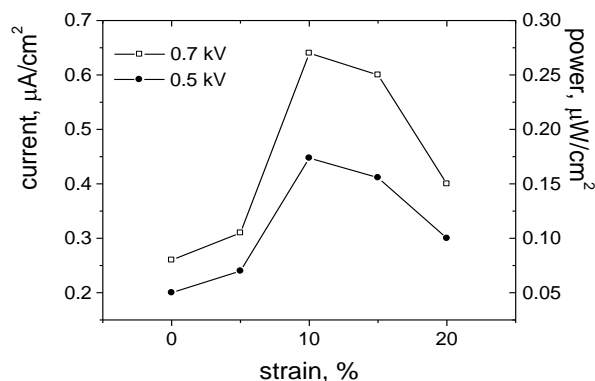


Fig. 6. Current through flexible energy harvesting with BaSrTiO<sub>3</sub> films sputtered at different voltages and the corresponding power densities.

Due to the high Young modulus of BST of 105 GPa [39], the films are brittle. It seems that sputtered BST films at 0.5 kV and 0.7 kV have the same critical point of the maximum allowable strain that they can withstand no matter of the crystallinity degree and perovskite phase presence. Initially, with the strain increase, the piezoelectric voltage and current also increased. Beyond a strain of 10%, the output power decreased, probably due to the work conditions near the tensile strength of the films (considering also their thickness), causing their degradation. Although this effect should be further studied by imaging the continuity of the films at different strains, at this stage it could be noted that the current and voltage decreased in the strain range 10-20%. It was previously found that for piezoelectric ceramics the tensile strengths do not increase with decreasing grain size [40], therefore it is not surprising the similar trend of the curve for both films.

Comparison with some of the most popular publications in the field, including lead-containing material with similar piezoelectric coefficients and design (Table 3) revealed that the proposed BST based energy harvesting element exhibited great potential for vibrational energy conversion by using thinner films and smaller size of the harvesting element in comparison with the reported in the literature.

The power density is comparable and in some cases even exceeding the reported, considering the difference in the functional film area and the operational frequency remains in the low-frequency range.

Table 3. Comparison of the energy harvesting performance of elements with a similar design, involving materials with a similar piezoelectric coefficient.

| Lead – free materials | Film thickness, μm | Power density, μW/cm <sup>2</sup> | Frequency, Hz | Area, cm <sup>2</sup> |
|-----------------------|--------------------|-----------------------------------|---------------|-----------------------|
| CYTOP [41]            | 15                 | 0.28                              | 37            | 2.33                  |
| AlN [42]              | 1                  | 0.038                             | 204           | 0.1                   |
| PZT [43]              | 1                  | 0.32                              | 183           | 0.77                  |
| This work             | 0.52               | 0.27                              | 50            | 0.40                  |

## Conclusion

Thin films of barium strontium titanate were deposited by magnetron sputtering. The variation of the deposition conditions results in tuning their desired piezoelectric properties. The film morphology, crystallinity, bond types and chemical states were shown to depend on the sputtering voltage. XPS investigation of the BaSrTiO<sub>3</sub> film sputtered at 0.7 kV reveals that perovskite phase has been formed. The polycrystalline nature and the typical absorption bands for perovskite phase are confirmed for this film by SEM and FTIR. A simple single layer energy harvesting element was designed and fabricated. Higher piezoelectric voltage and power density were measured in comparison with the device implementing BaSrTiO<sub>3</sub> film sputtered at a lower voltage of 0.5 kV, making the former films suitable for the above mentioned application. Future work will be related to study the effect of the film thickness for BST produced at the optimal sputtering voltage (0.7 kV) on the piezoelectric energy harvesting performance.

## Acknowledgments

This research was funded by the Bulgarian National Science Fund, grant DH 07/13. The authors acknowledge Prof. Armin Götzhäuser for the provided XPS facility.

## Conflicts of interest

There are no conflicts to declare.

## Keywords

Barium strontium titanate, energy harvesting, piezoelectric properties, sputtering voltage.

Received: 23 March 2020

Revised: 22 April 2020

Accepted: 04 May 2020

## Supporting information

There are no supporting information at the journal website.

## References

- Uchino, K.; Chapter 5 - Piezoelectric energy harvesting systems with metal oxides; Vu, Y. (Ed.); Elsevier: Netherlands, **2018**, pp. 91-126.
- Denishev, K; *J. Phys.: Conf. Ser.*, **2016**, 764, 012003.
- Gupta, S.; Heidari, H.; Lorenzelli, L.; Dahiya, R.; 2016 IEEE International Symposium on Circuits and Systems (ISCAS), Montreal, QC, pp. 345-348, **2016**.
- Jiang, B.; Iocozzia, J.; Zhao, L.; Zhang, H.; Harn, Y.-W.; Chen, Y.; Lin, Z.; *Chem. Soc. Rev.*, **2019**, 48, 1194.

5. Biglar, M.; Gromada, M.; Stachowicz, F.; Trzepieciński, T.; *Acta Mechanica et Automatica*, **2017**, *11*, 275.
6. Narita, F.; Fox, M.; Mori, K.; Takeuchi, H.; Kobayashi, T.; Omote, K.; *Smart Materials and Structures*, **2017**, *26*.
7. Shirakov, V.; Shakhovoy, R.; Pan'kin, A. V.; Kalinchuk, V. V.; *IOP Conf. Series: Mat. Sci. Eng.*, **2018**, *324*, 012006.
8. Wang, X.; Shi, J.; Piezoelectric Nanogenerators for Self-powered Nanodevices. In: *Piezoelectric Nanomaterials for Biomedical Applications. Nanomedicine and Nanotoxicology*; Springer, Berlin, Heidelberg, **2012**.
9. Manika, G. C.; Psarras, G. C; 2nd Hellenic Conference on Chemical Engineering, Athens, Greece, May 29-31, **2019**.
10. Kwon, S. R.; Huang, W. B.; Zhang, S. J.; Yuan, F. G.; Jiang, X. N.; *J. Micromech. Microeng.* **2016**, *26*, 045001.
11. Aleksandrova, M.; Dobrikov, G.; Kolev, G.; Marinov, Y.; Vlahov, T.; Denishev, K.; 41st International Spring Seminar on Electronics Technology (ISSE), Zlatibor, Serbia, 16-20 May **2018**.
12. Yu, S.; Zhang, C.; Wu, M.; Dong, H.; Li, L.; *J. Pow. Sourc.*, **2019**, *412*, 648.
13. Yu, S.; Li, L.; Zhang, W.; Suna, Z.; Zheng, H.; *J. Mat. Chem. C*, **2015**, *3*, 5703.
14. Aleksandrova, M.; Kolev, G.; Vucheva, Y.; Pathan, H.; Denishev, K.; *Appl. Sci.*, **2017**, *7*, 890.
15. Aragchi, M. E. A.; Shaban, N.; Bahar, M.; *Mat.Sci.– Poland*; **2016**, *34*, 63.
16. Phan, T. T. M.; Chu, N. C.; Luu, V. B.; Xuan, H. N.; Phan, D. T.; Martin, I.; Garriere, P.; *J.Sci.: Adv. Mat. Dev.*, **2016**, *1*, 90.
17. Aal, A. A.; Hammad, T. R.; Zaqrwah, M.; Battisha, I. K.; Hammad, A. B. A.; *Acta Physica Polonica A*, **2014**, *126*, 1318.
18. Seo, S. S. A.; Lee, H. N.; Noh, T. W.; *Thin Solid Films*, **2005**, *486*, 94.
19. Dai, Y. Y.; Chen, W. P.; Pang, G. K. H.; Lee, P. F.; Lam, H. K.; Wu, W.B.; Chan, H. L. W.; Choy, C. L.; *Appl. Phys. Lett.*, **2003**, *82*, 3296.
20. Ashiri, R.; *Vibrational Spectroscopy*, **2013**, *66*, 24.
21. Shen, Z.; Wu, Z.; Yao, Z.; Luo, D.; Cao, M.; Chen, W.; Xu, Q.; Zhou, J.; Liu, H.; *Ferroelectrics*, **2017**, *357*, 58.
22. Mahajan, S.; Thakur, O. P.; Prakash, Ch.; Sreenivas, K.; *Bull. Mater. Sci.*, **2011**, *34*, 483.
23. Reynolds, G.J.; Kratzer, M.; Dubs, M.; Felzer, H.; Mamazza, R.; *Materials (Basel)*, **2012**, *5*, 575.
24. You, Z.Z.; Hua, G.J.; *J. Alloys Comp.*, **2012**, *530*, 11.
25. Ayouchi, R.; Martin, F.; Ramos – Barrado, J. R.; Leinen, D.; *Surf. Interface Anal.*, **2000**, *30*, 565.
26. Rodrigues, A.; Bauer, S.; Baumbacha, T.; *Ceram. Inter.*, **2018**, *44*, 16017.
27. Xu, Y.; Tang, Z.; Zhang, Zh.; *Key Eng. Mat.*, **2008**, *368-372*, 535.
28. Fuentes, S.; Chavez, E.; Padilla-Campos, L.; Diaz-Droguett, D.E.; *Ceram. Int.*, **2013**, *39*, 8823.
29. Craciun, V.; Singh, R. K.; *Appl. Phys. Lett.*, **2000**, *76*, 1932.
30. Li, Y.; Wang, C.; Yao, Z.; Kim, H. K.; Kim, N. Y.; *Nanoscale Res. Lett.*, **2014**, *9*, 530.
31. Kim, Y. S.; Yun, D. J.; Kim, S. H.; Kyoung, Y. K.; Heo, S.; *Curr.Appl. Phys.*, **2016**, *16*, 1464.
32. Yu, Q.; Liu, D.; Wang, R.; Feng, Zh.; Zuo, Zh.; Qin, S.; Liu, H.; Xu, X.; *Mater. Sci. Eng. B*, **2012**, *177*, 639.
33. Nasser, S. A.; *Appl. Surf. Sci.*, **2000**, *157*, 14-22.
34. Rodrigues, A.; Bauer, S.; Baumbacha, T.; *Ceram. Inter.*, **2018**, *44*, 16017.
35. You, Z.Z.; Hua, G.J.; *J. Alloys Comp.*, **2012**, *530*, 11.
36. Briscoe, J.; Jalali, N.; Woolliams, P.; Stewart, M.; Weaver, P. M.; Cain M.; Dunn, S.; *Energy Environ. Sci.*, **2013**, *6*, 3035.
37. Chen, K.-H.; *Power Management Techniques for Integrated Circuit Design*, John Wiley & Sons, Singapore, **2016**.
38. Yeo, H.; Young, C.; Jeong, G.; *Compos. Part B:Eng.*, **2019**, *168*, 58.
39. Singh, S. N.; Measurement of elastic modulus of alumina and barium strontium titanate wafers produced by tape casting method, Technical Report ARMET-TR-12039, **2014**.
40. Ichikawa, H.; Ishikawa, T.; *Compr. Compos. Mater.*, **2000**, *1*, 107.
41. Suzuki, Y.; Edamoto, M.; Kasagi, N.; Kashwagi, K.; Morizawa, Y.; Micro electrets energy harvesting device with analogue impedance conversion circuit Proc.PowerMEMS'08, pp 7–10, **2008**.
42. Basrour, S.; Charlot, B.; Marzencki, M.; Grasso, A.; Colin, M.; Valbin, L.; DTIP '05 Symp., Scientific Commons, Montreux, Switzerland, pp. 299–302, **2005**.
43. Shen, D.; Park, J.-H.; Noh, J. H.; Choe, S.-Y.; Kim, S.-H.; Wikle III, H. C.; Kim, D.-J.; *Sens. Actuators A: Phys.*, **2009**, *154*, 103.

#### Authors biography



**Mariya Aleksandrova** received her MSc degree in electronics and the Ph.D. degree in the technology of electronic manufacturing from the TU-Sofia, in 2007 and 2010, respectively. Since 2015, she is an Associate Professor with the Department of Microelec–tronics, TU-Sofia. She is an author or co-author of 6 books and more than 80 papers in international journals and conference proceedings. Her current research interests include microelectronic technologies, MEMS, piezoelectric energy harvesting, flexible electronics.

**Tatyana Ivanova** received her MSc degree in physics from the Sofia University and PhD degree from Bulgarian Academy of Sciences. Currently, she is an Assoc. Prof. – researcher with CL-SENES, BAS. Her main interests are solid state physics, thin film materials, electrochromic effect, solar energy, FTIR and Raman spectroscopy. She is an author and co-author of more than 100 papers.

**Sascha Koch** worked as a technology specialist for Endress+Hauser, Maulburg, Germany in the period 2012-2015. Later, in the period 2015-2018, he was a researcher at the Faculty of Physics, Bielefeld University. Since 2019, he is an R&D Engineer at ETO Sensoric GmbH, Nürnberg, Germany. His research interests are XPS characterization, molecular assemblies, dynamic force microscopy. He is an author and co-author of more than 20 papers in international journals.

**Frank Hamelmann** received his MSc degree and Ph.D. degree in experimental physics, in 1995 and 1999, respectively. Currently, he is Professor in physics with the Bielefeld University. His scientific interests are thin film technologies, CVD, PVD, metal oxides. He is an author and co-author of more than 70 papers in international journals and conference proceedings.

**Daniela Karashanova** is head of Electron Microscopy Laboratory with the IOMT, BAS. Her research interests are materials characterization, nanomaterials, composites, thin films. She is an author and co-author of more than 100 papers in international journals and conference proceedings.

**Kostadinka Gesheva** received her MSc degree in physics of semiconductors from Faculty of Physics at Sofia University in 1968. She defended PhD dissertation at CL SENES-BAS in 1984 and received her DSc degree in 2008 in the field of electrical, magnetic and optical properties of condensed matter. She worked as a professor in CL-SENES, BAS and currently she is an associated member-professor. Her main research interests are semiconductors, solid state spectroscopy, solar energy, thin films, CVD. She is an author and co-author of more than 200 papers.

#### Graphical abstract

Energy harvesting device with an active area of 4 cm<sup>2</sup>, involving lead-free barium strontium titanate film with thickness ~ 500 nm produces stable piezoelectric voltage and electrical power of microwatt, sufficient to power supply low-power consuming electronic device.

